

# Measurement by Laser Induced Fluorescence on miscible density driven flows in a Hele–Shaw cell: settings and preliminary results

Jon Mainhagu\*, Constantin Oltéan, Fabrice Golfier, Michel A. Buès

Laboratoire environnement, géomécanique et ouvrages – ENSG – INPL, Nancy-Université, rue du Doyen Marcel-Roubault, BP 40,  
54501 Vandœuvre-lès-Nancy, France

Received 18 May 2006; accepted after revision 30 January 2007

Presented by Michel Combarous

## Abstract

To be able to quantify concentration fields during a salt solute injection in a Hele–Shaw cell, an analogue medium to a porous media under specific conditions, an apparatus based on LIF technique has been set. This technique uses a diverged pulsed laser illuminating the cell in a light spot. To overcome the spatial and temporal light energy nonuniformity a data reduction involving the stacking of several consecutive rough images has been defined. This data reduction leads to a very good description of the mixing zone (finger) as well as both longitudinal and transversal concentration profiles. Comparison with another technique (light absorption) highlights the improvement our system provides both in precision and repeatability. *To cite this article: J. Mainhagu et al., C. R. Mecanique 335 (2007).*

© 2007 Académie des sciences. Published by Elsevier Masson SAS. All rights reserved.

## Résumé

**Mesures par LIF des écoulements miscibles dans une cellule Hele–Shaw : mise au point et résultats préliminaires.** Afin de quantifier les champs de concentration lors de l'injection d'une solution saline dans une cellule de type Hele–Shaw, représentant sous certaines conditions un modèle analogue à un milieu poreux, un banc de mesures basé sur une méthode LIF a été mis au point. Cette technique a impliqué l'utilisation d'un laser pulsé dont le faisceau défocalisé illumine la cellule sous la forme d'une tache laser. Afin de s'affranchir de la non uniformité spatiale et temporelle de l'intensité lumineuse de cette tache, un procédé de compilation de plusieurs images brutes successives a été envisagé. Ce traitement conduit à une description fine de la zone de mélange (doigt) et l'obtention des profils longitudinaux et transversaux en concentration. La comparaison avec une autre technique de mesure, basée sur l'absorption lumineuse, a souligné les améliorations apportés par notre système tant en termes de précision que de répétabilité. *Pour citer cet article : J. Mainhagu et al., C. R. Mecanique 335 (2007).*

© 2007 Académie des sciences. Published by Elsevier Masson SAS. All rights reserved.

**Keywords:** Fluid mechanics; Laser Induced Fluorescence; Miscible flows; Hele–Shaw cell

**Mots-clés :** Mécanique des fluides ; Fluorescence Induite par Laser ; Écoulement miscible ; Cellule Hele–Shaw

\* Corresponding author.

E-mail address: [jon.mainhagu@ensg.inpl-nancy.fr](mailto:jon.mainhagu@ensg.inpl-nancy.fr) (J. Mainhagu).

## 1. Introduction

Instability developments in density driven flows have been investigated in pseudo (or artificial) real porous media (stacked plastic spheres) [1]. This kind of study is unusual. Indeed, the problem with such systems is a less than exhaustive control over media parameters, such as local permeability. The slightest local heterogeneity can lead to unexpected fingering, due to the instable development of such a flow [2].

In order to acquire this control, previous works focused on the Hele–Shaw cell. Indeed, a Hele–Shaw cell allows one to get rid of local heterogeneities as well as presenting an analogy regarding flow in a porous media [3]. An analogy with transport has also been underlined by Taylor [4] and more recently by Oltéan et al. [5]. In this last paper, an important work compilation was made about the generalized form of the Taylor dispersion tensor in presence of a density/viscosity contrast. Up until now, studies mainly developed the qualitative aspect of flows. Experiences undertaken inside Hele–Shaw cell dealt with pattern recognitions [6] and global comportment of density driven interface [7]. A similar approach has been adopted for many other types of unstable flows, such as viscous fingering [8–10], thermal driven flows [11–13] or non-Newtonian fluids comportment [14,15]. We can therefore acknowledge that Hele–Shaw cells are often used as an analog experimental apparatus to characterize transport in porous media. It should be emphasized that these investigations are usually restricted to non miscible flows for which experiments are easier to put into practice.

As for miscible density driven flows in a Hele–Shaw cell, Fernandez [16] looked into it but only from an interface tracking point of view. Magnetic Resonance Imaging (MRI) technique was chosen by Johannsen et al. [17]. It is worth mentioning that some of these works present reduced measurements but generally do not focus on it. Felder [18] set up an experimental apparatus based on light absorption in order to investigate, from a quantitative point of view [5,18], the behaviour of the mixing zone obtained by the injection of a salt solution. So, in accordance with the experimental conditions, two different spatial solute evolutions can be obtained. The first one can be assimilated to that of a so-called finger while the second one with two fingers. Consequently, in order to simplify the writing and to be in accordance with the overall shape, we will replace ‘mixing zone’ by ‘finger’ hereafter. Our goal is to improve the understanding of finger formation, following Felder’s work.

The choice for new experimental measurement techniques can achieve such a goal. We chose to utilize Laser Induced Fluorescence (LIF) as a mean to measure concentration fields. LIF is a well known technique regarding concentration measures in fluids. This technique can also lead to temperature fields [19]. As far as we know, this technique has never been carried out with a Hele–Shaw cell. The illumination of a cell by a laser has already been used as a coherent light source, but not, as in our case, as excitation energy source for a fluorescent dye [13].

First we will describe the apparatus and the experimental method put together to obtain concentration field measurements. Choices made to optimize the experimental system will also be discussed. We will then present some results and deal with repeatability and error margin issues. We will finish by presenting a quick comparison with the previous results on longitudinal and transversal concentration profiles.

## 2. Experimental apparatus and method

Experiments were performed in a Hele–Shaw cell. The cell consists of two parallel transparent plates disposed vertically and placed in an aluminum enclosure which is used to set the width between the glass plates of the cell to 0.5 mm. Note that this aperture fixes the intrinsic permeability of the analog porous medium. The plates are made of optical glass 300 mm in height, 200 mm wide and 10 mm thick. A needle placed inside the cell was used for the injection (inner diameter = 0.25 mm, outer diameter = 0.46 mm). The needle was connected to a step by step motored push syringe.

The measurement technique involved is Laser Induced Fluorescence (LIF), a technique described, for example by Wang [20], based on the excitation of a fluorescent dye included in the studied fluid, in our case Rhodamine 6G. The system include both a double cavity pulsed laser (wavelength at 535 nm, 12 mJ per pulse) and a 12 bits definition digital camera as the recording device. The camera is aimed perpendicular to the cell, but not the laser beam which is placed at one meter from the cell.

Within the experimental conditions presented here this technique raises additional difficulties. Adapting the LIF technique to the Hele–Shaw cell requires a different illumination than a standard LIF application as many have used (e.g., Herlina and Jirka [21]). Usually LIF is set with a laser plane that is perpendicular to the camera axis. In our case

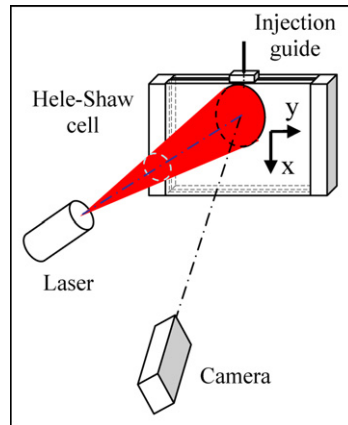


Fig. 1. Schematic of the laser beam divergence and cell lighting.

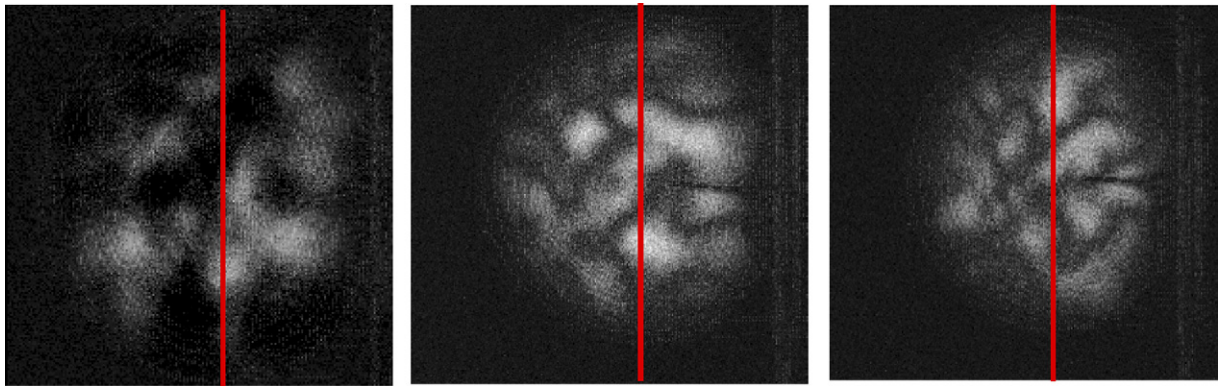


Fig. 2. Light intensity difference between two consecutive images (0.4 s between each images): three consecutive spots.

we cannot get a laser plane inside the Hele–Shaw cell. Consequently, as shown in Fig. 1, we have to diverge totally the laser beam so that when it hits the cell, we get a large spotlight on the required area. De facto, this specificity requires the consideration of two aspects of the light energy repartition of the laser. The spatial energy repartition is unstable over time and the light energy across a laser beam is not constant but rather has a Gaussian repartition vs. radius. This means that not only the energy level of the spot is non uniform but it also varies from pulse to pulse. If we visualize the intensity difference between two consecutive pulses (Fig. 2), we see non uniform energy level (dark and light areas). Moreover, these areas are not localized in the same place over time. They move from spot to spot. To be able to apply the LIF technique, these two aspects have to be compensated to obtain a rigorous measurement technique. It should be noted that we chose to work with a pulsed laser instead of a continuous one that is more common in LIF measures. As we will see in the closing statement, using this experimental apparatus also allows us to perform velocity measures which require a pulsed laser. Moreover, a continuous laser would present the same pattern as a pulsed one, only attenuated, so using one would not cancel the problem.

The spatial energy variation implies that the same zone will not be illuminated with the same intensity on two consecutive images. In order to overcome this effect, we have to define a measure as a stack of consecutive images. When we use an average image resulting from ten consecutive rough images we obtain a much better mean repartition. To see explicitly the modification, we injected a small quantity of Rhodamine in the cell and illuminate it with the laser spot. We can choose an axis across the spot and then extract the light intensity repartition from the difference between two consecutive images. Fig. 3 shows this exploitation, done from four couples of rough images (a) and from four couples of averaged images (b). Average images are ten consecutive images taken in 4.5 seconds and stacked into one. This is done two times in a row to get a couple of average images and we then visualize the difference between them. During the recording of the ten images we can consider the physical phenomenon to be in a quasi steady state.

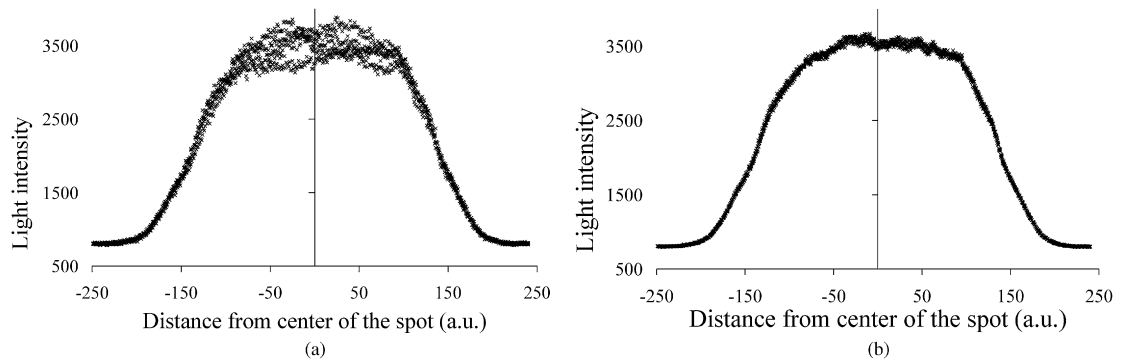


Fig. 3. Intensity across the light spot on the Hele–Shaw cell for four different couples of consecutive images. (a) Rough images considered. (b) Mean images considered.

We see that the curves from the averaged images are stable over time. Consequently the use of ten rough images to produce one mean image allows us to have an intensity profile that is constant throughout time.

These curves also show a modified Gaussian repartition of the intensity. This is due to the radial Gaussian intensity repartition across the laser beam and to the overall spot shape deformation (due to the aim angle of the laser). One way to take care of this is to set a different calibration for each pixel of the image. Indeed, thanks to the mean image procedure, each pixel of the camera will always receive the same light energy for a given concentration.

As our experimental measurement technique involves Rhodamine marking a salt solution, we have to be sure that salt will not have a significant impact on Rhodamine fluorescence. Both the intensity and the spectral response have to be considered. Regarding intensity, if we consider a salt concentration up to 10 g/L, the variation is less than 5%. From a spectral point of view, we have seen that the maximum intensity wavelength does not vary from a salt concentration of 10 g/L to a solution without salt. We can conclude that the presence of salt in the solution does not modify the Rhodamine compartment in our settings, i.e., the wavelength of the Rhodamine light emission as well as its intensity.

One last parameter to define is the dimension of the apparatus. In fact, the specific dimensions of the cell implies that, if we wish to analyze our results as a flow compartment inside a porous media regardless of the medium dimensions, we have to verify that the cell boundary conditions have no effect on any experiment. We have considered the upper boundary, linked to the penetration depth of the injection needle. Our measures have shown that the shape of the injection is not influenced by the upper cell boundary, for a needle penetration depth greater than 7 mm. Consequently, to get a reasonable margin, a needle penetration depth of 20 mm is used. This parameter also allows us to locate the light spot more effectively centered on the injection.

To get the best precision on the concentration measure we choose to use 3900 grey levels out of the 4095 maximum grey levels of the CCD camera and the aperture is wide open (4.8). These settings conduct to a Rhodamine concentration of  $6 \times 10^{-6}$  mole/L. This concentration has the other advantage to be relatively low, so that the Rhodamine will not be concentrated enough to fix itself on sensitive parts (e.g.: on the glass plates) and disrupt measures. It is important to bear in mind that this setting is also influenced by the distance between the camera and the cell. So, if specific measures have to be conducted closer to the cell, the optimal concentration may change.

As we see, the experimental apparatus has been optimised in order for the LIF technique to fit our needs. This setting was the first step, and now we can proceed looking into the actual experimental results.

### 3. Experimental results: comparison

The extracted concentration field presented in Fig. 4(a) shows a global shape of finger coherent with experimental and numerical results obtained in a real porous medium [21]. Both longitudinal and transversal profiles issue to data reduction should enable us to advance several physical interpretations about the salt solution behaviour. We can also compare results from our apparatus to those obtained previously with another technique that involved a commercial digital compact camera and a constant back lightning of the cell [18]. In [18] the salt solution was marked using a brilliant CFC blue dye and the measures were based on the absorption of the light by the dye according to the Beer–Lambert law: the more light is absorbed, the higher the concentration. Hereafter, we will refer to our apparatus as ‘LIF’ and to the digital camera apparatus as ‘absorption’.

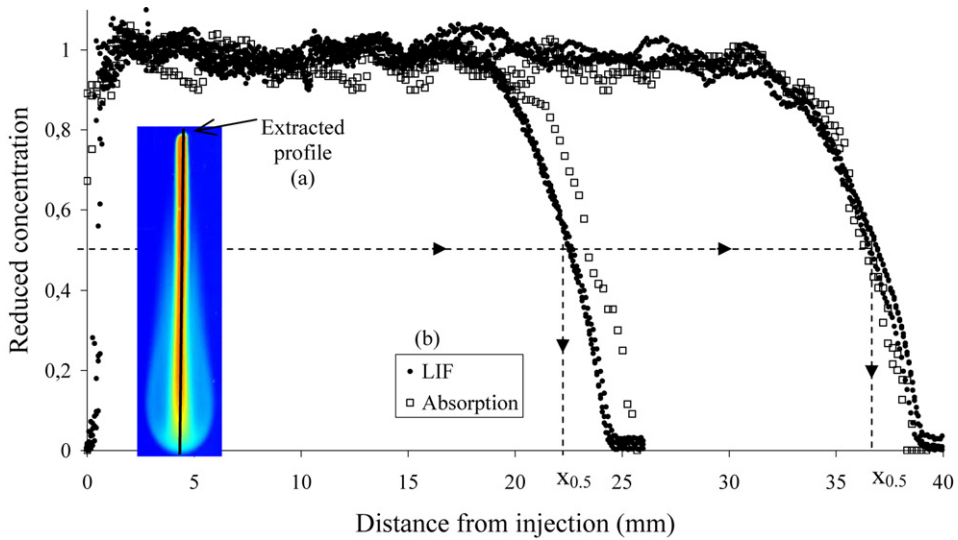


Fig. 4. (a) Finger visualization using LIF and (b) longitudinal reduced concentration profiles ( $C_{inj} = 1$  g/L,  $Q_{inj} = 0.5$  mL/h at 5 and 8 min)—comparison between LIF and absorption.

We compare first the longitudinal profiles ( $x$ -direction) obtained for an injected salt-solute concentration of  $C_{inj} = 1$  g/L at a flow rate of  $Q_{inj} = 0.5$  ml/h, after 5 and 8 minutes of injection. We consider reduced concentration ( $C/C_{inj}$ ) for these profiles. Using these settings led to the development of a single finger (Fig. 4(a)). The longitudinal profile, along the injection axis, shown Fig. 4(b), underlines a few preliminary conclusions:

- (i) The shape of reduced concentration profiles along the longitudinal section for both LIF and absorption measures are coherent. More specifically, we can see that advance fronts display a similar dispersion. We acknowledge that both measurement systems presented identical results within each specific precision. LIF measures also present a good repeatability, indeed for each time, three LIF profiles are displayed.
- (ii) In the finger central section, experiences (although overall undisplayed) prove that the reduced concentration quickly becomes steady and suggests, as mentioned in [21], the presence of a stable core. So, we can divide the finger into two parts along the mean flow direction: the upper part and the lower—more diffusive—part.

In addition, the advance front, on the lower part, is presented in Fig. 5 illustrating specifically the reduced concentration versus reduced length at different times. Since repeatability is good, we only visualize one profile for each time. The reference length is the distance between the injection point and the profile position for  $C/C_{inj} = 0.5$  at considered time (Fig. 4(b)), noted  $x_{0.5}$ . We see that the reduced diffusive fronts are equivalent between LIF and absorption measures. The slopes of the curves are compatible when compared for the same time. Nevertheless, the LIF curves present a more regular bending. One last point can be underlined. In reduced co-ordinates the advance profile slope straightens when time increases. A similar behaviour has been pointed out in globally 1D displacement breakthrough curves [23].

Regarding Fig. 6, we visualize several transversal profiles ( $y$ -direction) at a given time for different section, each section being defined by a reduced length, i.e.:  $S_i = x_i/x_{0.5}$ .  $x_i$  is the length where the section is extracted, so we will use the notation  $S_i$  to define the reduced length. On each graph is shown both LIF and absorption reduced concentrations. Again, as in Fig. 4(b), three LIF profiles are displayed for each section. The transversal profiles allow us to complete the previous observations deduced above, as follows:

- (i) Close to the injection point ( $S_1$ ), the measures show a ‘piston’ displacement. Advection phenomenon prevails. Even if it is not entirely shown here, for lower transversal profile sections (see  $S_2$  and  $S_3$ ), we have identical curves along the upper part. In addition Fig. 7, that displays longitudinal profiles across time for a fixed section ( $x = 22$  mm), shows for the upper part a steady profile along the length. At 5 min the profile is at the lower part

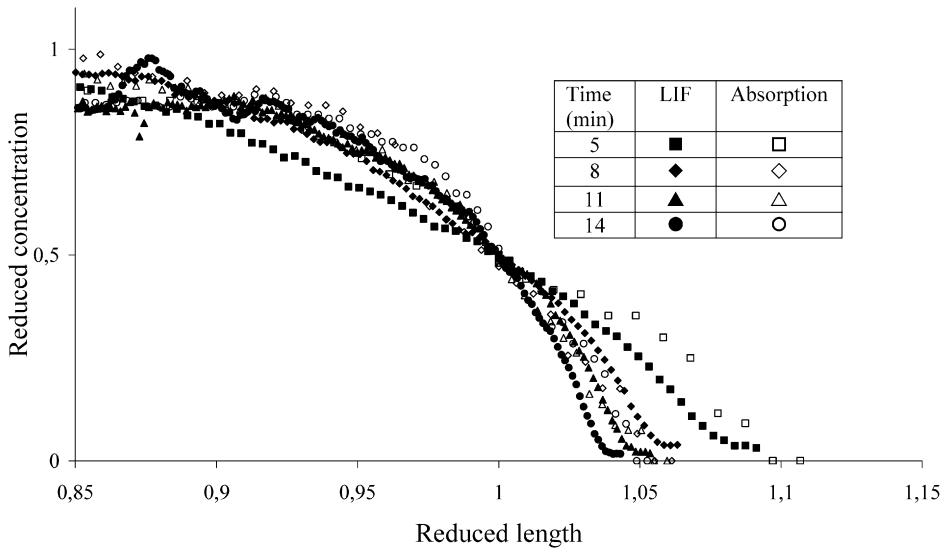


Fig. 5. Lower part of longitudinal concentration profiles ( $C_{inj} = 1 \text{ g/L}$ ,  $Q_{inj} = 0.5 \text{ mL/h}$ ) LIF and absorption.

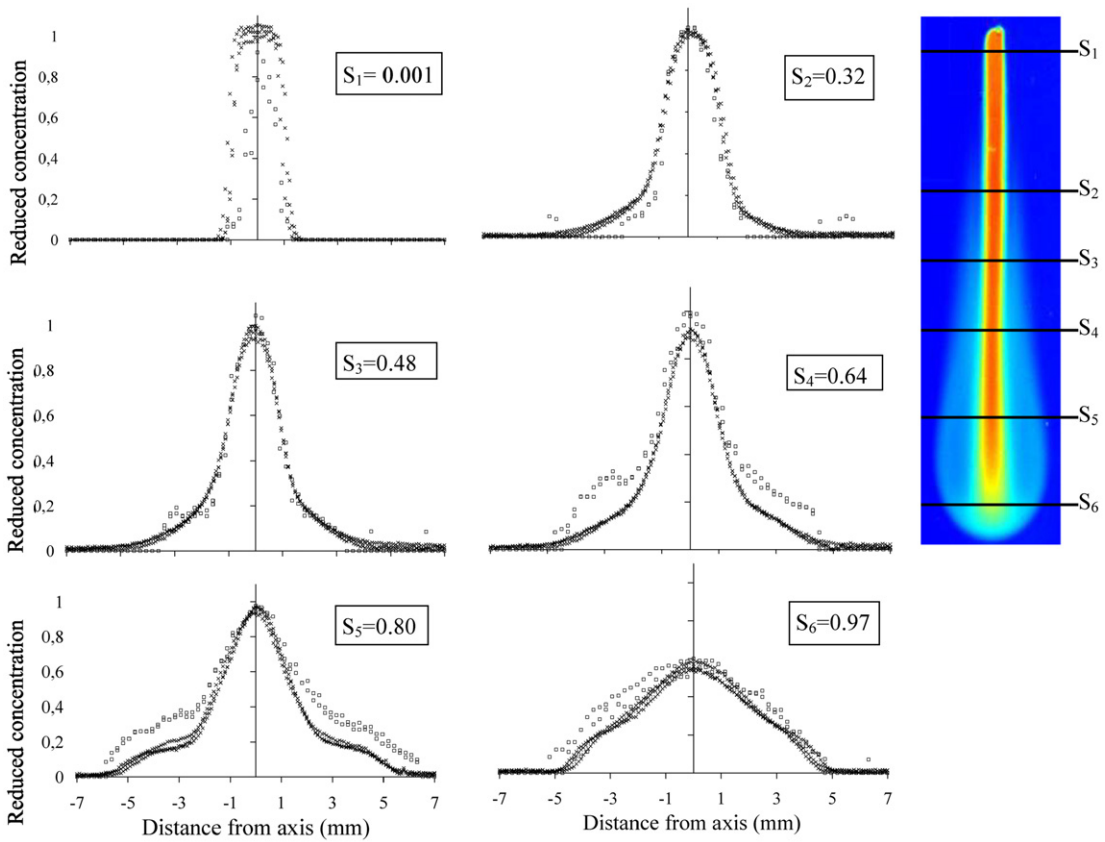


Fig. 6. Transversal concentration profiles ( $C_{inj} = 1 \text{ g/L}$ ,  $Q_{inj} = 0.5 \text{ mL/h}$  at 14 min) for six sections—comparison between LIF (x) and absorption (□).

of the injection, but after 9 min, we acknowledge the transversal profile to maintain its shape around the axis. We can experimentally concur with Oltéan and Buès [22] in the observation regarding a stable core in the upper part.

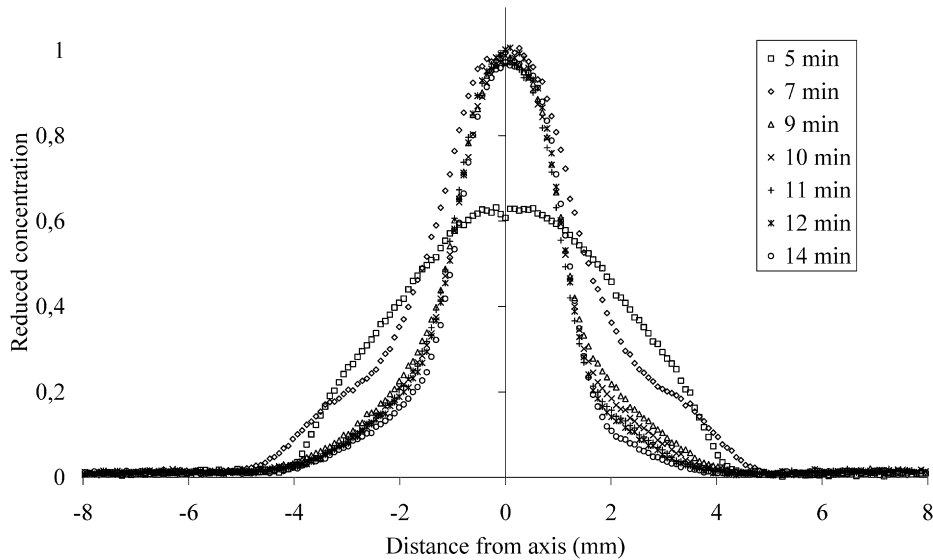


Fig. 7. Transversal concentration profile ( $C_{inj} = 1 \text{ g/L}$ ,  $Q_{inj} = 0.5 \text{ mL/h}$ ) at several times for the section  $x = 22 \text{ mm}$ .

- (ii) The lower part of the injection reveals the different compartment foreseen above. Sections  $S_4$  to  $S_6$  show a lateral dispersion that did not occurred on the upper part.  $S_5$  shows the apparition of an inflexion of the profile. Moreover,  $S_6$  underlines the transversal profile of the advance front. This distinctive deportment can be explained with the existence of convective cells on opposite sides of the injection finger. Their presence controls the development of the lower part. The presence of these cells has been already numerically shown [21]. To experimentally prove it, velocity measures have to be set. In each of these graphs, the comparison between LIF and absorption measures denotes a clear compatibility. On the lower part, dispersion transport becomes predominant. These profiles also underline a difference between LIF and absorption measures. Localized away from the axis, the absorption measurements present slightly higher concentrations than the ‘LIF’ ones. As we said above, this zone is predominantly dispersive. The lack of accuracy and reproducibility at low concentration lead us to believe that the absorption technique present some difficulties to be as accurate as LIF in low concentration.

Although measurements using the two techniques seem to be similar, the better accuracy and good reproducibility of the LIF based measures are obvious. These superiorities come from two main improvements:

- (i) We obtain a much larger number of points for curves. In order to display 10 mm LIF measures uses 169 pixels as opposed to the 46 pixels used by the photographic measures. This leads to a precision improvement by a factor greater than 3.5, so the rise of the number of points gives us much-detailed curves. This greater resolution allows us greater precision when getting information out of those curves. For example, the longitudinal dispersion and the finger velocity displacement terms, which can be extracted from the curve of the advance front using momentum method, will now have greater accuracy. The standard deviation for absorption measure is also three times the one for LIF. The steady part of the curve is therefore much better defined.
- (ii) The main achievement for these measures is a major sensitivity improvement. Indeed, the photographic measure gets 256 grey levels to describe reduced concentration from zero to 1. The LIF gets 3900 grey level. Combined with a fluorescent dye that enables a much more precise calibration, which allows us to see the fine structure of the transversal curves that we could not clearly get before. This sensitivity improvement is also well served by the control provided on the incident laser lightning, allowing a much more constant behaviour of the fluorescent dye.

#### 4. Conclusion and perspectives

In this Note, we have seen a way to setup an experimental apparatus around a Hele–Shaw cell involving the LIF technique. The issues raised by this choice have been addressed and optimised in order for the measurements to

be the most effective. A comparison of results helped acknowledge that measures are improved. More accurate and more precise experiments can now be set into motion. This improvement will now be put to use, as to determine the physical aspect behind the development of multiple digitations in density driven injection in a Hele–Shaw cell. The extraction of useful information from measurements will include front velocity, but also experimental values of both longitudinal and transversal dispersion coefficients. These measures will help apprehending the apparition of multiple fingers from an experimental point of view with a wide range of parameters, and therefore help raising a valid experimental conclusion.

As [5] allows us to get numerical simulation of the same physical phenomenon, we will also be able to put together a joined experimental and numerical study. This comparison will lead to the improvement of the numerical code as well as an added source of information for the analysis of the apparition of multiple fingers.

The next step will be to determine simultaneously, both concentration and velocity fields. As we also realised, the existence of anti-clockwise rotation convective cells have to be experimentally proven, which is only possible through velocity field measures. In order to achieve this, PIV technique will be set alongside, using the same laser used as for the LIF settings now fully operational.

## References

- [1] M. Rosen, V.M. Freytes, A. D’Onofrio, C.A. Allain, J.P. Hulin, Density difference driven instabilities in porous media, *Granular Matter* 3 (2001) 63–67.
- [2] R.A. Schincariol, Dispersive mixing dynamics of dense miscible plumes: Natural perturbation initiation by local scale heterogeneities, *Journal of Contaminant Hydrology* 34 (3) (1998) 247–271.
- [3] J. Martin, N. Rakotomalala, D. Salin, Gravitational instability of miscible fluids in a Hele–Shaw cell, *Physics of Fluids* 14 (2) (2002) 902–905.
- [4] G.I. Taylor, Dispersion of a soluble matter in solvent flowing slowly through a tube, *Proceeding of the Royal Society of London A* 219 (1953) 186–203.
- [5] C. Oltéan, C. Felder, M. Panvilov, M.A. Buès, Transport with a very low density contrast in Hele–Shaw cell and porous medium: Evolution of the mixing zone, *Transport in Porous Media* 55 (2004) 339–360.
- [6] C. Bizon, A.A. Predtechensky, J. Werne, K. Julien, W.D. McCormick, J.B. Swift, H.L. Swinney, Dynamics and scaling in quasi-two-dimensional turbulent convection, *Physica A* 239 (1997) 204–210.
- [7] S.E. Pringle, R.J. Glass, C.A. Cooper, Double diffusive finger convection in a Hele–Shaw cell: An experiment exploring the evolution of concentration fields, length scales and mass transfer, *Transport in Porous Media* 47 (2002) 195–214.
- [8] R. Wooding, Growth of fingers at an unstable diffusing interface in a porous medium or Hele–Shaw cell, *Journal of Fluid Mechanics* 39 (3) (1969) 477–495.
- [9] E. Pitts, Penetration of fluid into a Hele–Shaw cell: The Saffman–Taylor experiment, *Journal of Fluid Mechanics* 97 (1) (1980) 53–64.
- [10] M. Kawaguchi, K. Makino, T. Kato, Viscous fingering patterns of silica suspensions in polymer solutions: effects of viscoelasticity and gravity, *Physica A* 246 (1997) 385–398.
- [11] J.W. Elder, Transient convection in a porous medium, *Journal of Fluid Mechanics* 27 (1967) 609–623.
- [12] M. Ozawa, U. Müller, I. Kimura, T. Takamori, Flow and temperature measurement of natural convection in a Hele–Shaw cell using a thermo-sensitive liquid–crystal tracer, *Experiments in Fluids* 12 (1992) 213–222.
- [13] J. Mihailovic, C. Beckermann, Development of a two-dimensional liquid species concentration measurement technique based on absorptiometry, *Experimental Thermal and Fluid Science* 10 (1995) 113–123.
- [14] S. Obernauer, G. Drazer, M. Rozen, Stable–unstable crossover in non-Newtonian radial Hele–Shaw flow, *Physica A* 283 (2000) 187–192.
- [15] A. Boschan, V.J. Charette, S. Gabbanelli, I. Ippolito, R. Chertoff, Tracer dispersion of non-Newtonian fluids in a Hele–Shaw cell, *Physica A* 327 (2003) 49–53.
- [16] J. Fernandez, Density driven unstable flows of miscible fluids in a Hele–Shaw cell, *Journal of Fluid Mechanics* 451 (2002) 239–260.
- [17] K. Johannsen, S. Oswald, R. Held, W. Kinzelbach, Numerical simulation of three-dimensional saltwater–freshwater fingering instabilities observed in a porous medium, *Advances in Water Resources* (2006), in press.
- [18] C. Felder, Transport d’une solution saline en cellule de Hele–Shaw—Expériences et simulations numériques, PhD thesis, Institut National Polytechnique de Lorraine, 2003.
- [19] P. Lavieille, F. Lemoine, M. Lebouché, G. Lavergne, Mesure de la température de gouttelettes en combustion par fluorescence induite par laser à deux couleurs : résultats préliminaires et perspectives, *C. R. Acad. Sci. Paris Série IIb* 329 (2001) 557–564.
- [20] G. Wang, On high spatial resolution scalar measurement with LIF Part 1, *Experiments in Fluids* 29 (2000) 257–264.
- [21] Herlina, G.H. Jirka, Application of LIF to investigate gas transfer near the air–water surface in a gris-stirred tank, *Experiments in Fluids* 37 (2004) 341–349.
- [22] C. Oltéan, M.A. Buès, Infiltration of salt solute in homogeneous and saturated porous media—an analytical solution evaluated by numerical simulations, *Transport in Porous Media* 48 (2002) 61–78.
- [23] J.M. Strauss, M.A. Buès, Réduction d’échelle en hydrodynamique des milieux poreux : application à l’étude du transfert d’un micropolluant métallique, in: 9<sup>ème</sup> Congrès Français de Mécanique, 1989, pp. 120–121.